Science Advances
AAAS

advances.sciencemag.org/cgi/content/full/7/12/eabe5940/DC1

Supplementary Materials for

Catalytic amplification by transition-state molecular switches for direct and sensitive detection of SARS-CoV-2

Noah R. Sundah, Auginia Natalia, Yu Liu, Nicholas R. Y. Ho, Haitao Zhao, Yuan Chen, Qing Hao Miow, Yu Wang, Darius L. L. Beh, Ka Lip Chew, Douglas Chan, Paul A. Tambyah, Catherine W. M. Ong, Huilin Shao*

*Corresponding author. Email: huilin.shao@nus.edu.sg

Published 17 March 2021, *Sci. Adv.* **7**, eabe5940 (2021)
DOI: 10.1126/sciadv.abe5940

This PDF file includes:

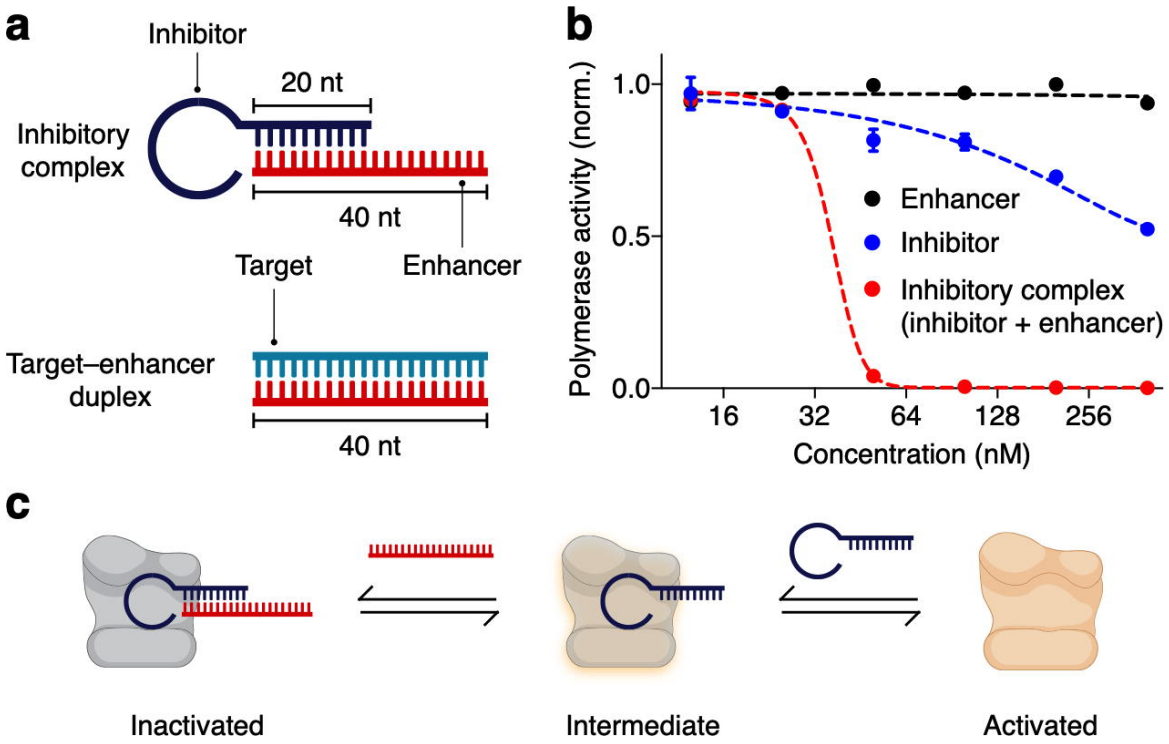

Supplementary Figure 1. Polymerase activity of multicomponent molecular switches. **(a)** Schematic representation of the inhibitory complex. The complex consists of an inhibitor and an enhancer strand. While only half of the enhancer strand (20 nucleotides) can hybridize with the inhibitor strand, it is designed to be fully complementary (all 40 nucleotides) with the target, making the formation of the target–enhancer duplex thermodynamically favored. Within the inhibitory complex, half of the enhancer strand remains single-stranded so that its displacement by the target is kinetically favored. **(b)** Inhibitory effects of the different molecular switch constituents on polymerase activity. The inhibitor strand alone weakly decreases the polymerase activity, while the addition of the enhancer strand strongly inhibits the polymerase activity. The enhancer strand by itself does not demonstrate any appreciable inhibitory effect. **(c)** Schematic representation of the dynamic equilibrium between different forms of the molecular switches (i.e., inactivated, intermediate and activated). All measurements in **b** were performed in triplicate, and the data are presented as mean ± s.d.

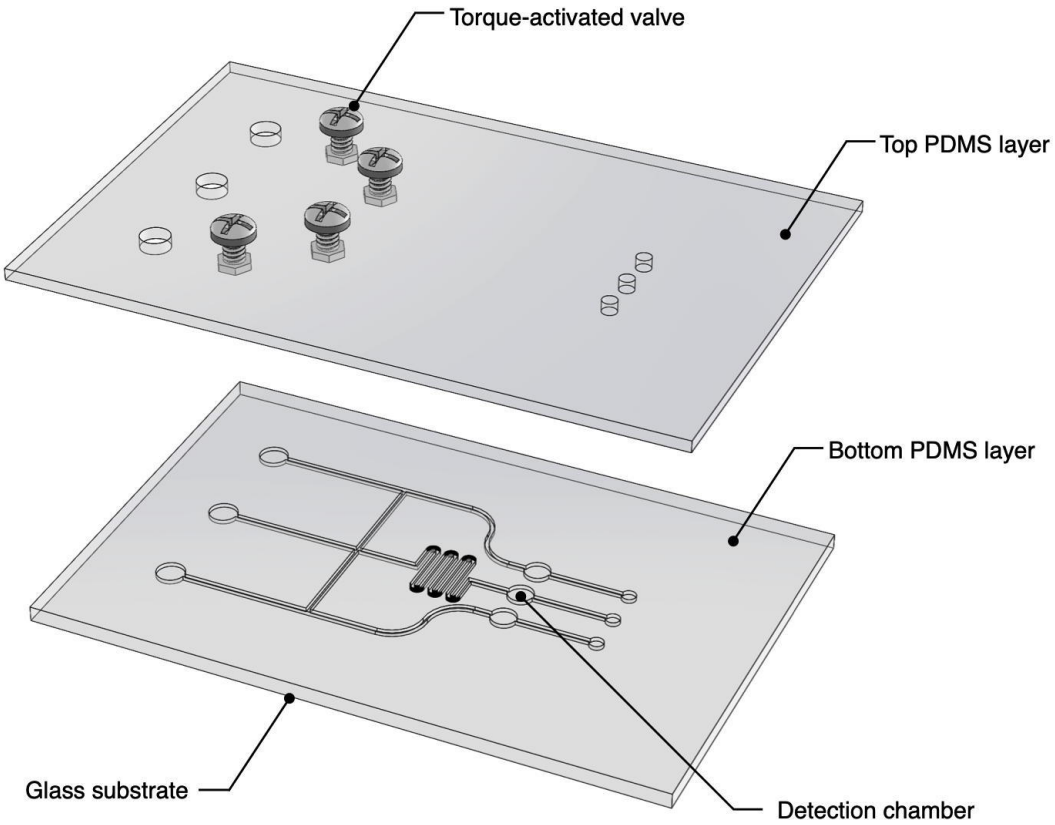

Supplementary Figure 2. Exploded view of the microfluidic device.
The platform was assembled from two polydimethylsiloxane (PDMS) layers on a glass substrate, with torque-activated valves for sequential flow control.

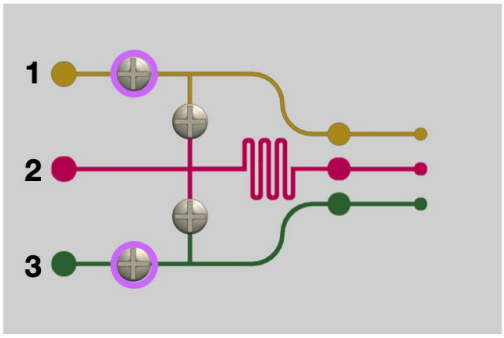

Step 1: Sample loading and target recognition

- Samples are introduced into the inlets, reconstituting the lyophilized reagents in the device.
- By opening the valves (purple), samples flow into the detection chambers.

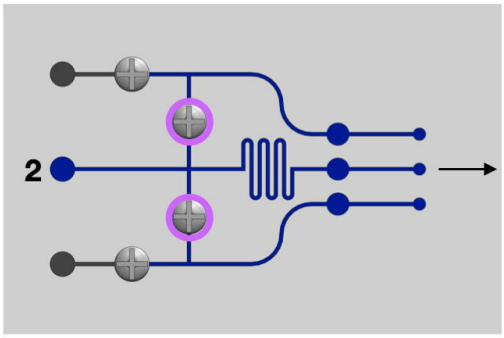

Step 2: Enzymatic amplification

- Excess reagent mixtures are removed via the waste outlet.
- By opening the valves (purple), streptavidin-conjugated HRP is introduced through inlet 2.

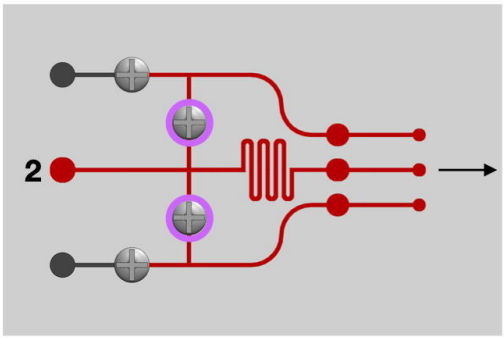

Step 3: Fluorescence detection

- Unbound HRP is removed and HRP substrate is introduced through inlet 2 into the detection chambers by opening the valves (purple).
- On-chip, smartphone-based fluorescence measurements are performed to detect HRP substrate development.

Supplementary Figure 3. Operation of the microfluidic CATCH platform.

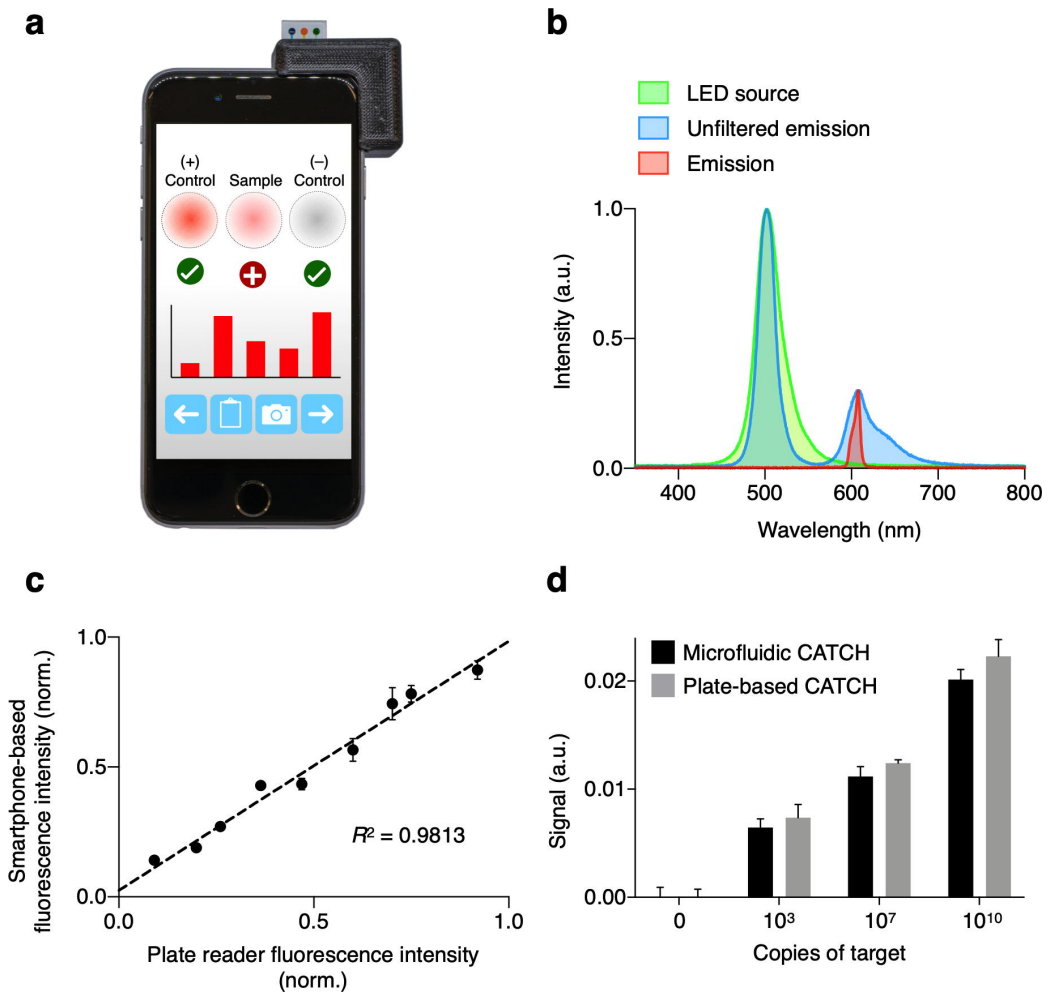

Supplementary Figure 4. Portable CATCH assay.

(a) Photograph of the smartphone-based fluorescence detector. **(b)** Optical spectra of the LED source, unfiltered and filtered fluorescence emission. **(c)** Correlation of the smartphone-based detector and conventional plate reader. The smartphone-based detector correlates well with the commercial reader (R^2 = 0.9813). **(d)** CATCH assay performance in microfluidic and plate format. The CATCH assay in its microfluidic chip format demonstrated good consistency with the assay in its plate format. All measurements were performed in triplicate, and the data are presented as mean ± s.d. in **c** and **d**. a.u., arbitrary unit.

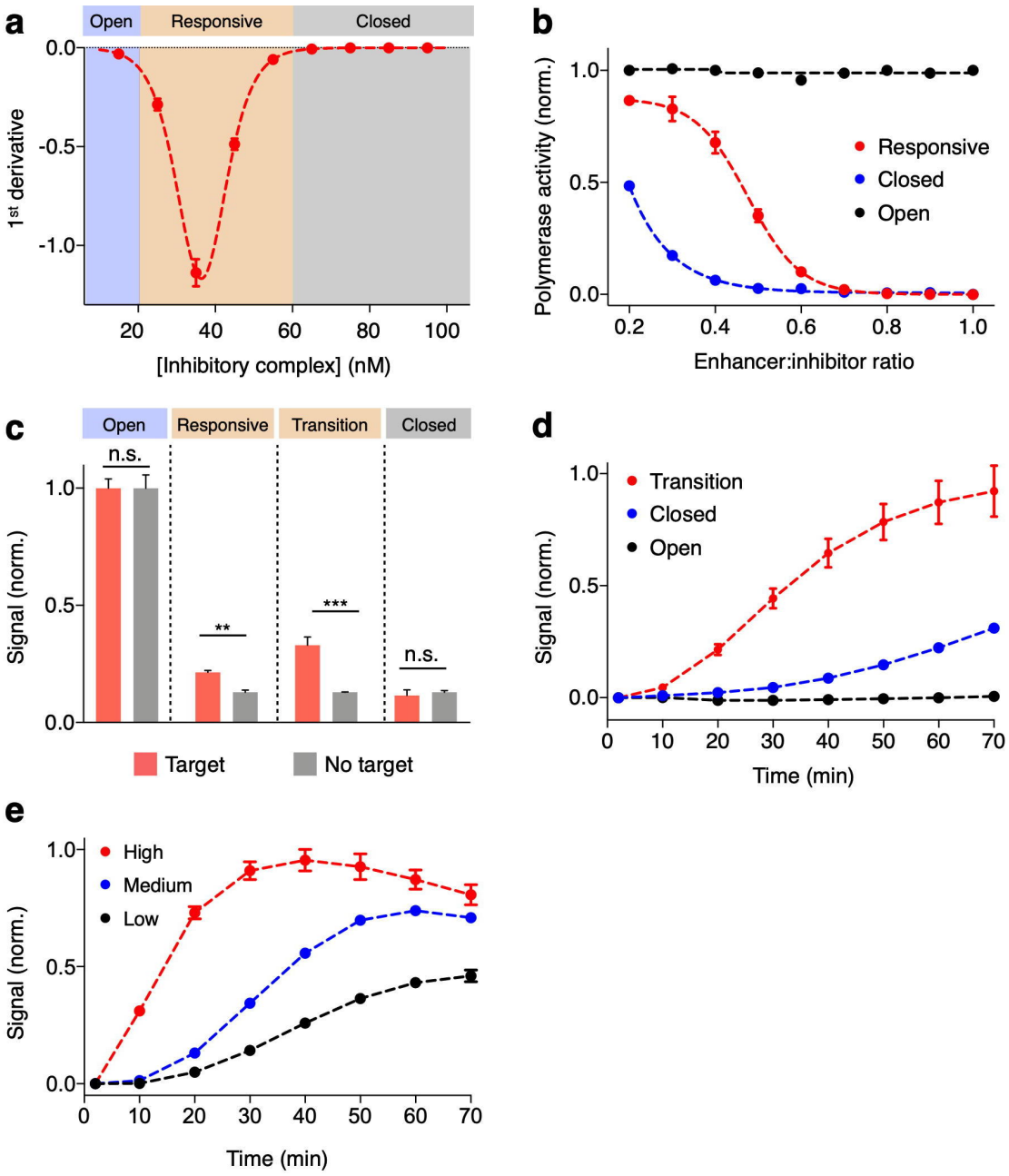

Supplementary Figure 5. Performance characterization of the transition-state molecular switches.

(a) First derivative plot of the inhibition curve to illustrate switch responsiveness to inhibitory complex. Molecular switches were prepared with a varying concentration of the inhibitory complex. Based on the resultant changes in polymerase activity, we categorized molecular switches into three groups: open, responsive, and closed. In the responsive range, molecular switches are responsive to changes in the inhibitory complex concentration. When the inhibitory complex concentration is above this range, molecular switches are in the closed state, where most switches are inactivated. When the inhibitory complex concentration is below this range, molecular switches are in the open state, where switches are predominantly activated. **(b)** Perturbation of the responsive-, closed- and open-state molecular switches. Molecular switches were perturbed by reducing the ratio of enhancer:inhibitor. Responsive-state molecular switches could not only react to a broader range of perturbations, but also respond with bigger changes in their polymerase activity. **(c)** Signal evaluation of the transition-state molecular switches. Molecular switches of different states were incubated with or without target for 30 minutes at room temperature and the

resultant polymerase activity was measured. The transition-state molecular switches showed further signal improvement over the responsive-state switches, while the closed- and open-state switches failed to produce any distinguishable signal. **(d)** Activation kinetics. When incubated with SARS-CoV-2 N-gene target at room temperature, the transition-state molecular switches achieved the fastest activation kinetics. **(e)** Signal generation kinetics. Transition-state molecular switches were activated with different target concentrations. Higher target concentration results in faster signal generation. Different molecular switches in **c**–**e** were prepared at the following representative compositions (inhibitor and enhancer strand, respectively): open state, 1 nM and 1 nM; transition state, 36 nM and 24 nM; closed state, 100 nM and 100 nM. All measurements were performed in triplicate and the data are presented as mean ± s.d. (***$P < 0.005$, **$P < 0.01$, n.s., not significant, Student's *t*-test).

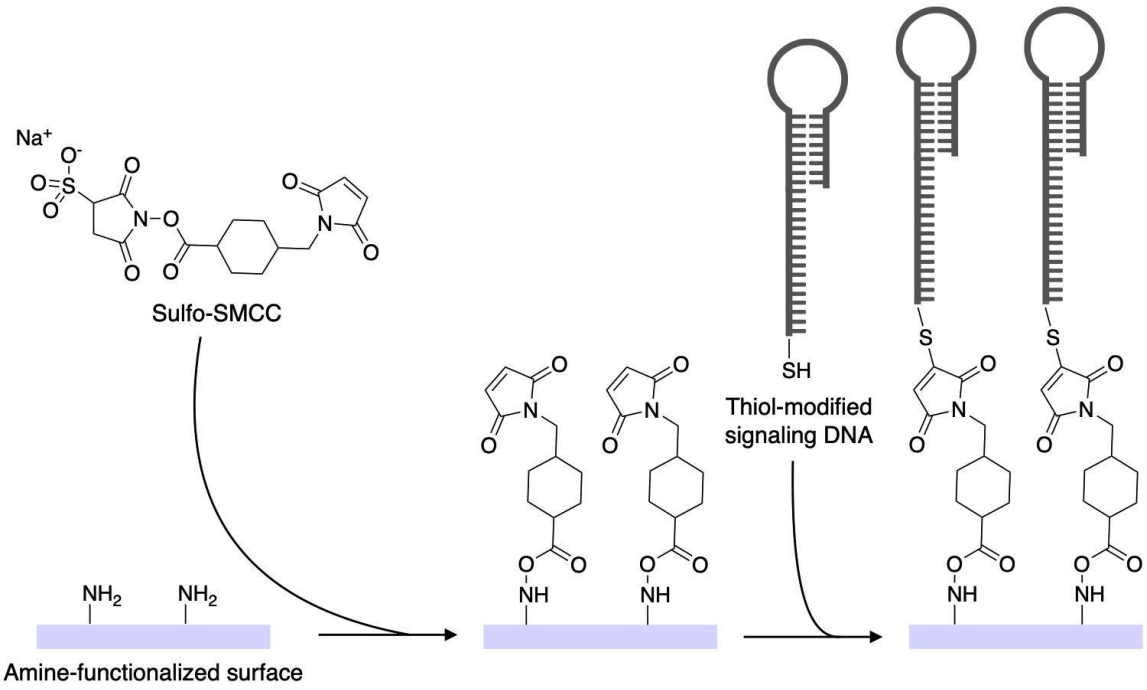

Supplementary Figure 6. Immobilization of signaling oligonucleotides.
We first functionalized different sensor surfaces with amine groups. Specifically, for the 96-well plate, bovine serum albumin (BSA) was coated onto the plate as an amine-rich protein scaffold; for the microfluidic device, (3-aminopropyl)triethoxysilane (APTES) was applied. Primary amines were then activated by incubating with sulfosuccinimidyl 4-(N-maleimidomethyl)cyclohexane-1-carboxylate (sulfo-SMCC). Separately, thiol-modified signaling oligonucleotides were activated by reducing the disulfide bonds. The activated oligonucleotides were then added to the amine-functionalized surface for covalent bonding.

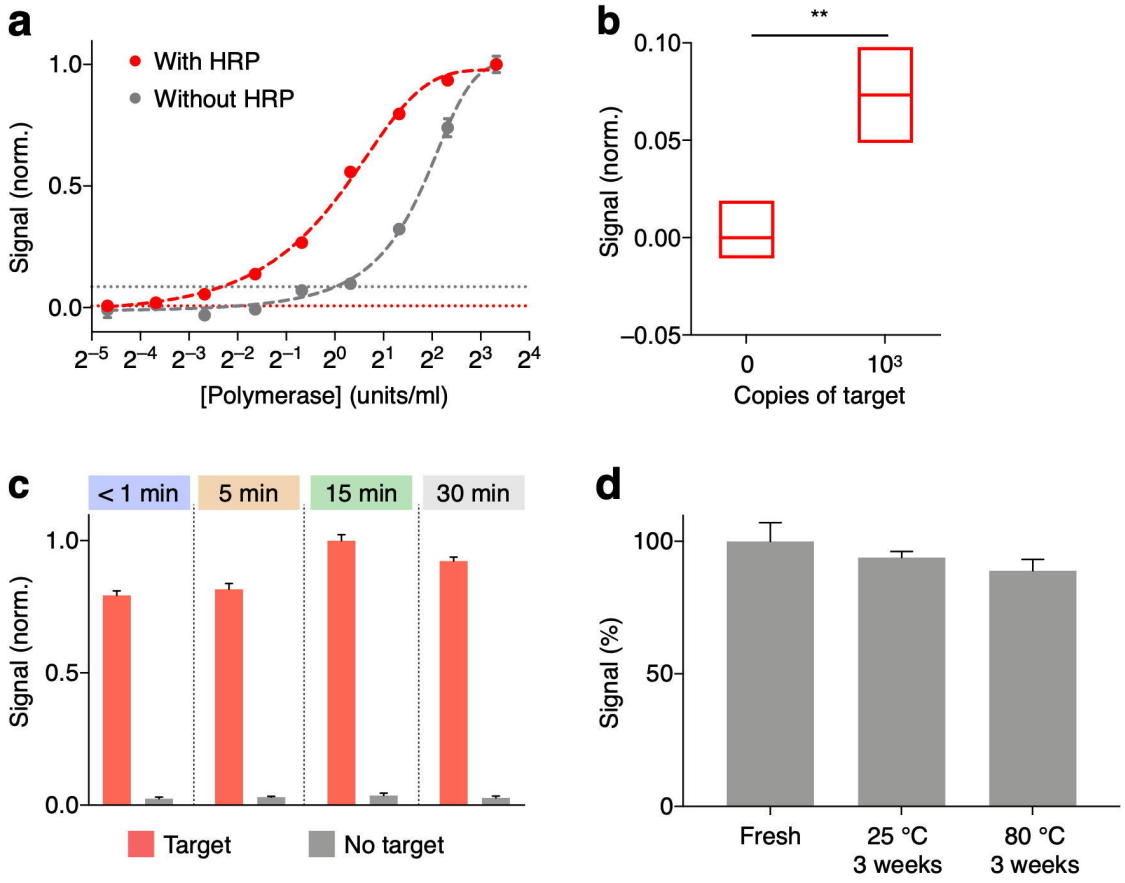

Supplementary Figure 7. CATCH signal amplification and portable integration.
(a) Improved performance through additional enzyme recruitment. Through the recruitment of an additional enzyme cascade (horseradish peroxidase, HRP), the CATCH assay generated fluorescence signals even at a low amount of polymerase activity. **(b)** CATCH performance with a low amount of target. Significant signal difference was observed between no-target control and 1,000 copies of target. **(c)** Lyophilization of molecular switch reagents. To facilitate portable applications, we lyophilized the CATCH reagents (i.e., molecular switch and biotin-modified dNTPs). The lyophilized reagents were then reconstituted for <1 min, 5 min, 10 min, and 30 min, before being mixed with target oligonucleotides. The lyophilized molecular switches demonstrated spontaneous assembly and preserved functionalities. **(d)** Accelerated aging of lyophilized molecular switches. Reagents were lyophilized and their activity measured after 3 weeks at room temperature (25 °C) and under accelerated aging (80 °C). All measurements were performed in triplicate, and the data are presented as mean ± s.d. (**$P < 0.01$, Student's *t*-test).

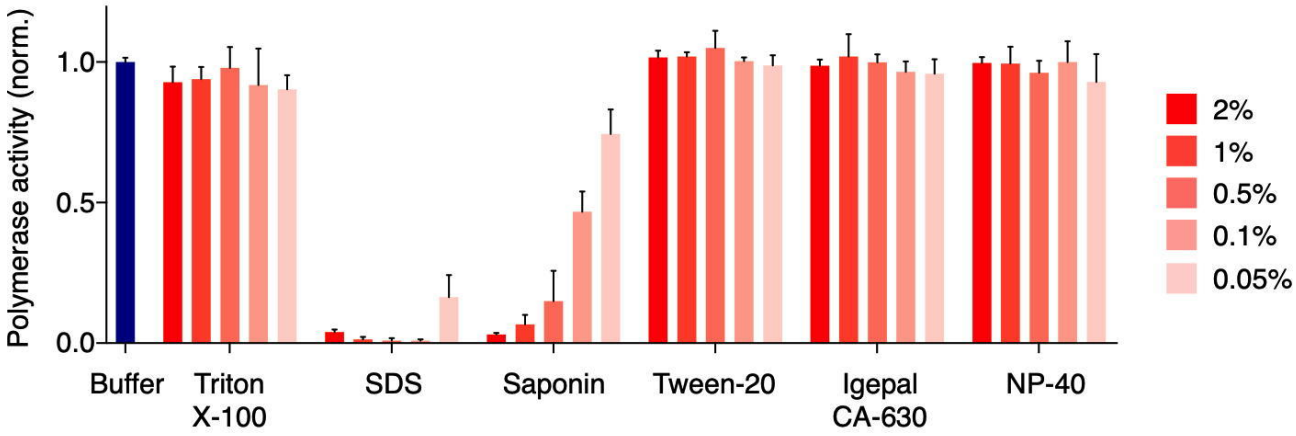

Supplementary Figure 8. Effects of detergents on polymerase activity.
Polymerase activity was evaluated in the presence of various concentrations of single detergents. Polymerase activity was highly inhibited in the presence of sodium dodecyl sulfate (SDS) and gradually inhibited with increasing concentration of saponin. The other detergents tested showed negligible effects on polymerase activity, regardless of their applied concentrations. All measurements were performed in triplicate and the data are presented as mean ± s.d.

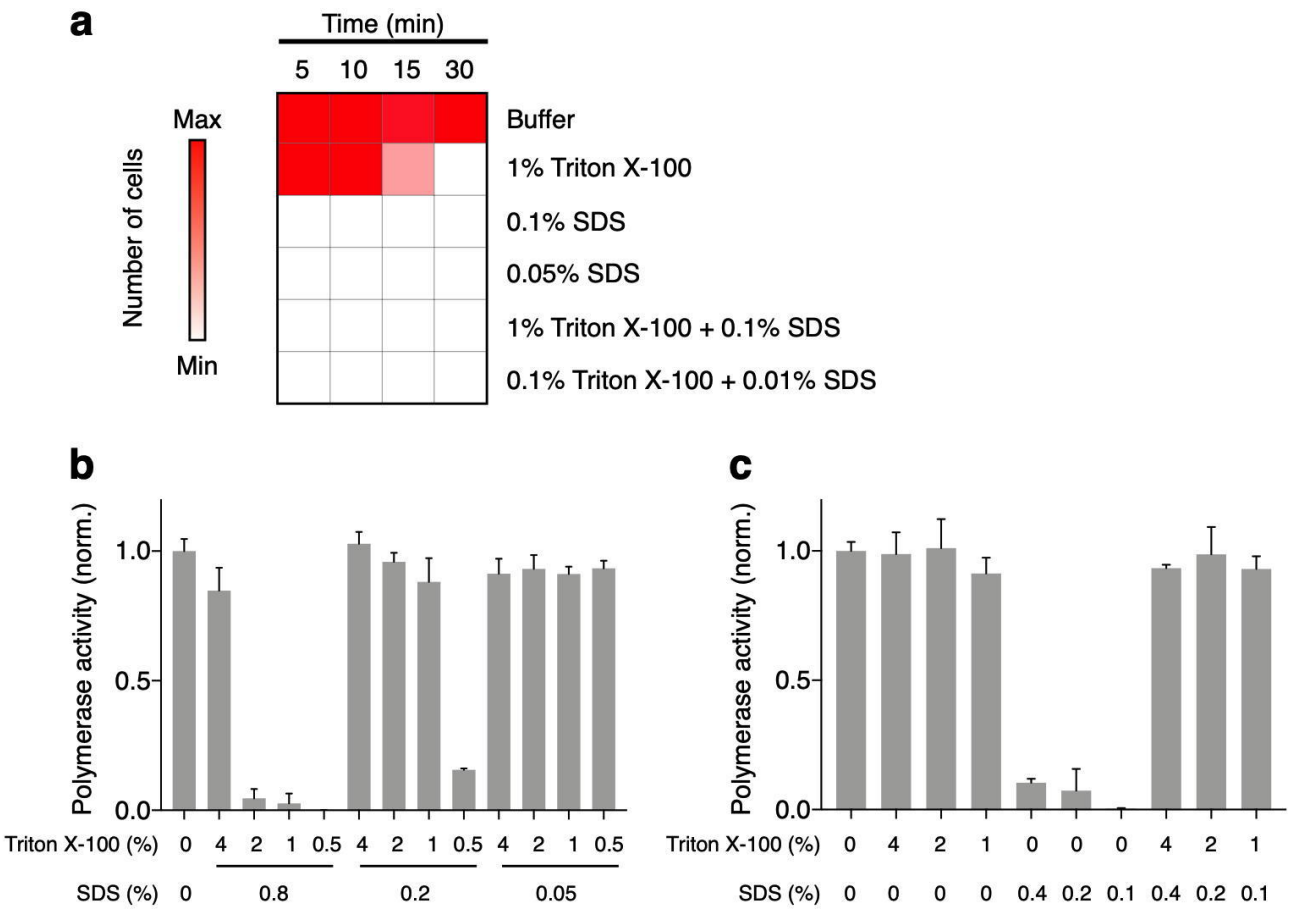

Supplementary Figure 9. Effects of detergents on cell lysing efficiency.
(a) Single or a mixture of detergents were used to lyse cells. All detergents, except 1% Triton X-100, could efficiently lyse cells within 5 minutes. **(b–c)** Polymerase activity was evaluated in the presence of various combinations of Triton X-100 and SDS. An optimal ratio of 1:10 between SDS and Triton X-100 could both preserve polymerase activity and lyse cells within 5 minutes. All measurements were performed in triplicate and the data are presented as mean in **a** and as mean ± s.d. in **b** and **c**.

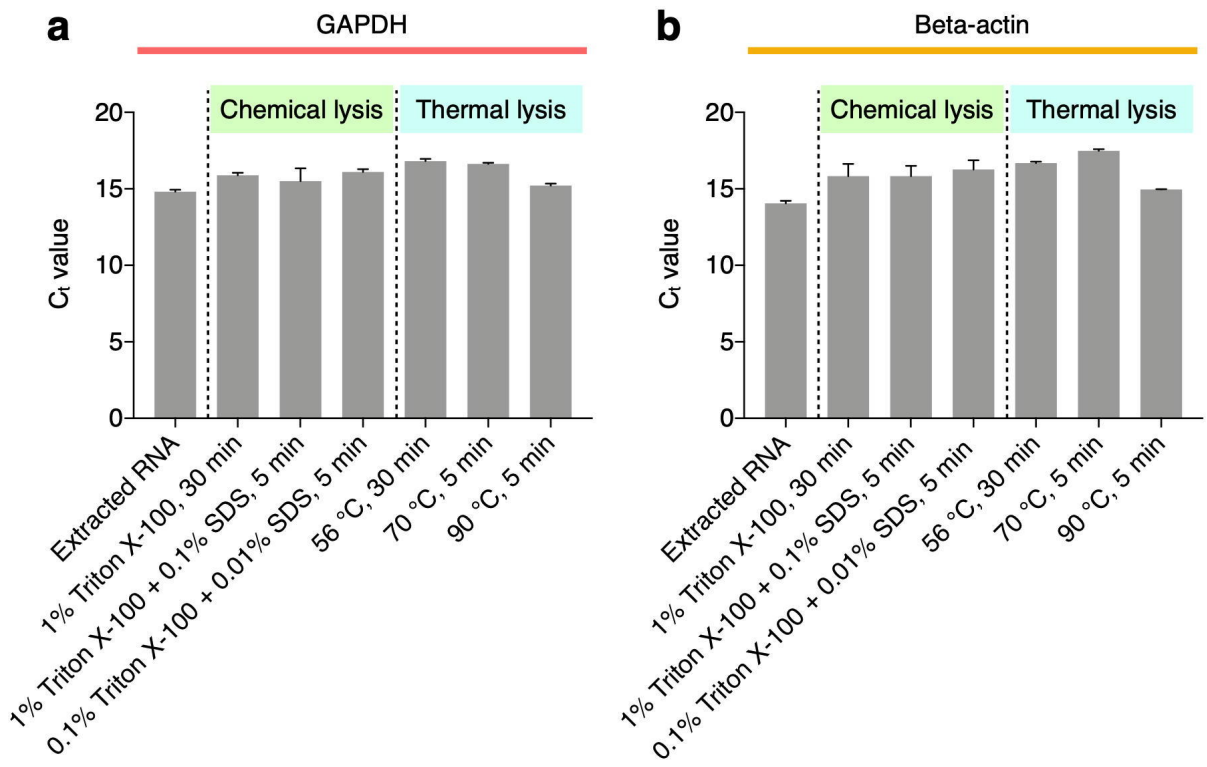

Supplementary Figure 10. Release and preservation of endogenous RNA targets by chemical and thermal lysis.

Endogenous mRNA targets GAPDH **(a)** and beta-actin **(b)** were measured in human lung epithelial cells. Gold-standard RNA samples were prepared from the cell culture through standard extraction. Chemical and thermal lysates were prepared respectively from an equivalent cell culture, without RNA extraction. All measurements were performed in triplicate, through RT–qPCR analysis. The lysis methods could effectively release and preserve endogenous RNA targets. The data are presented as mean ± s.d.

Supplementary Table 1. Oligonucleotide sequences.

Molecular switches	
SARS-CoV-2 S gene inhibitor	TTATTTGACTCCTGGTGATTCAATGTACAGTATTG
SARS-CoV-2 S gene enhancer	AATCACCAGGAGTCAAATAACTTCTATGTAAAGCAAGTAA
SARS-CoV-2 N gene inhibitor	AATCCATGAGCAGTGCTGACCAATGTACAGTATTG
SARS-CoV-2 N gene enhancer	GTCAGCACTGCTCATGGATTGTTGCAATTGTTTGGAGAAA
Signaling oligonucleotides	
Self-priming hairpin template	C**GG**C**G**TAC**G**TA**G**A**G**C**G**TT**G**A**G**CA**GG**AT**G**CCAACA**G**TC**G**ATCA**GG** AC**G**A**G**T**G**CTAACGCATTGTCGATAGCTCAGCTGTC TGAGCTATCGACAATGCGTT
Biotinylated dumbbell template	**GTGCGTACATAGATCGTTA**TCTGTCTAACGATCTATGTACGCACTC ACTCAGCTAACGCATTGTCGATAGCTCAGCTGTCTGAGCTATCGA CAATGCGTT
Mismatch analysis	
SARS-CoV-2 S gene synthetic target	GTTTCAAACTTTACTTGCTTTACATAGAAGTTATTTGACTCCTGGTG ATTCTTCTTCAGG
2 mismatch SARS-CoV-2 S gene synthetic target	GTTTCAAACTTTACTTGCTTTACATAGAAGTTCTTTGACTCCTGATG ATTCTTCTTCAGG
4 mismatch SARS-CoV-2 S gene synthetic target	GTTTCAAACTTTACTTGCTTTACATAGAAGTTCTTGGACTCATGATG ATTCTTCTTCAGG
6 mismatch SARS-CoV-2 S gene synthetic target	GTTTCAAACTTTACTTGCTTTACATAGAAGCTCTTGGAATCATGATG ATTCTTCTTCAGG
8 mismatch SARS-CoV-2 S gene synthetic target	GTTTCAAACTTTACTTGCTTTACATAGAAGCTCTGGGAATCATGATG AGTCTTCTTCAGG

10 mismatch SARS-CoV-2 S gene synthetic target	GTTTCAAACTTTACTTGCTTTACATAGAAGCTCTGGGAATCAGGATTAGTCTTCTTCAGG
12 mismatch SARS-CoV-2 S gene synthetic target	GTTTCAAACTTTACTTGCTTTACATAGAAGCTCTGGGTATCAGGATTAGGCTTCTTCAGG

Bolded nucleotides indicate possible sites of biotin incorporation/removal.

Underlined nucleotides indicate mismatches.